**Philip S. Marcus**
Professor
Department of Mechanical Engineering,
University of California,
Berkeley, CA 94720-1740
e-mail: pmarcus@me.berkeley.edu

**Xylar Asay-Davis**
Center for Nonlinear Studies,
Los Alamos National Laboratory,
Los Alamos, NM 87545
e-mail: xylar@lanl.gov

**Michael H. Wong**
e-mail: mikewong@astro.berkeley.edu

**Imke de Pater**
Professor
e-mail: imke@berkeley.edu

Department of Astronomy,
University of California,
Berkeley, CA 94720

# Jupiter's Red Oval BA: Dynamics, Color, and Relationship to Jovian Climate Change

*Jupiter now has a second red spot, the Oval BA. The first red spot, the Great Red Spot (GRS), is at least 180 yr old. The Oval BA formed in 2000 was originally white, but part turned red in 2005. Unlike the Great Red Spot, the red color of the Oval BA is confined to an annulus. The Oval's horizontal velocity and shape and the elevation of the haze layer above it were unchanged between 2000 and 2006. These observations, coupled with Jupiter's rapid rotation and stratification, are shown to imply that the Oval BA's 3D properties, such as its vertical thickness, were also unchanged. Therefore, neither a change in size nor velocity caused the Oval BA to turn partially red. An atmospheric warming can account for both the timing of the color change of the Oval BA as well as the persistent confinement of its red color to an annulus.* [DOI: 10.1115/1.4007666]

*Keywords: Jupiter, chaotic mixing, climate change, vortices, secondary circulations, zonal winds, red oval*

## 1 Two Unsolved Problems of the Jovian Atmosphere

One unsolved problem of the dynamics in Jupiter's atmosphere is how heat is transported in its weather layer; another is the unexpected change in color of one of its long-lived vortices. Here, we define the *weather layer* as the layer in the troposphere that is bounded above by the tropopause and below by the top of its underlying convective zone. We define the convective zone as that region of the Jovian atmosphere that is *fully* convective with a nearly adiabatic vertical lapse rate. The weather layer, as we have defined it, has a subadiabatic lapse rate with a well-defined (real) Brunt–Väisälä frequency. Local "weather" within the weather layer can include intermittent and locally confined convectively driven storms, which are sometimes made visible by lightning [1], but, on average, the weather layer is both baroclinically and convectively stable. The stability is what leads to the most visible aspect of the weather layer: the cloud tops associated with its persistent vortices such as the GRS.

The unsolved heat-transfer problem associated with the weather layer is that Jupiter, like Earth, receives more incident radiation from the Sun at its equator than at its poles. However, unlike Earth, the average cloud-top temperature in the weather layer is approximately the same: 110 K at 150 mbar at all latitudes [2]. The transport mechanism that moves the solar energy deposited at the equator to the poles remains unknown.

The unsolved color change problem occurred in the Oval BA. The Oval BA is Jupiter's second largest (after the GRS [3]) persistent vortex with a major axis of nearly 8000 km. Like the GRS, it is an anticyclone (i.e., spinning counterclockwise in the southern hemisphere). The Oval BA formed in 1998–2000 from the mergers of three other anticyclones (see Sec. 1.2), and after its formation, its visible cloud tops were white. Then, starting in December 2005 and over the span of a few months, the clouds in an annular ring within the vortex turned red, while those interior to and exterior to the ring remained white (see Figs. 1 and 2). The red annulus has persisted from 2006 to the present time.

In this paper, we expand our earlier hypothesis [4] that the mergers of the three vortices that created the Oval BA disrupted the *global* heat transfer from the Jovian equator to its poles resulting in temperature changes in the weather layer's cloud tops of order 5–10 K. We further expand our earlier arguments [5–10] that this Jovian-wide temperature change was responsible for the formation and persistence of the red annulus in the Oval BA. Our hypothesis of a global temperature change could be easily supported or refuted if the *absolute* temperature of the cloud tops were measured. However, despite the fact that the *relative* temperatures (with respect to other parts of the atmosphere) of the Jovian cloud tops have been made frequently, the *absolute* temperatures (which are needed to determine if there were significant temperature changes between 2000 and 2006) have not been made. As

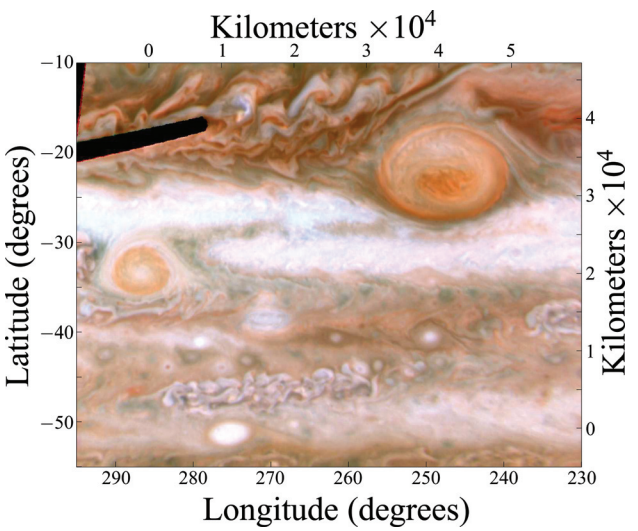


**Fig. 1 Planetographic HST map (435, 502, and 658 nm) of Jupiter on April 24, 2006. The Oval BA and Great Red Spot are at 33 °S and 23 °S, respectively. Kilometer scales are approximate because they vary with latitude.**

Manuscript received November 8, 2010; final manuscript received September 7, 2012; published online December 6, 2012. Assoc. Editor: Akshai Runchal.

  

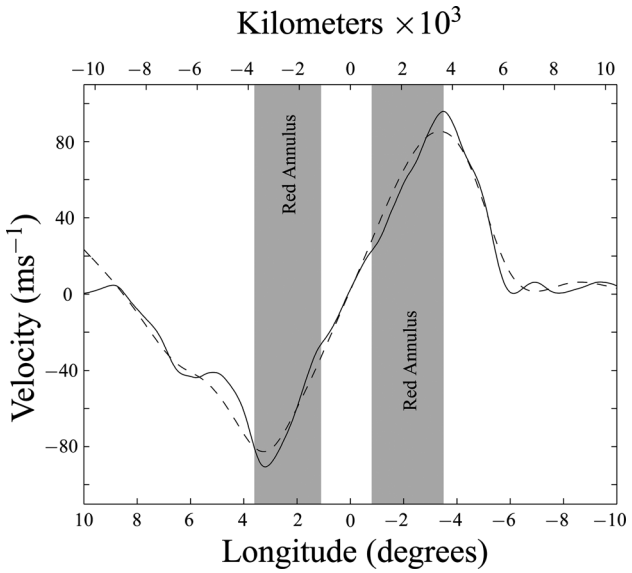


**Fig. 2 North–south velocities along the east–west axis (33°S) of the Oval BA in 2006 (solid line) when it had a red annulus and in 2000 (broken line) when it was all white; mean velocity uncertainties are 5.5 m/s and 3 m/s, respectively. At the peaks, the differences between the curves are greater than these uncertainties due to differences in resolution and to smoothing in the velocity-extraction algorithms [42]. Velocities are from HST (658 nm, April 24–25, 2006) and Cassini (December 11–13, 2000). Gray shading indicates the location of the red annulus in 2006–2008. The "bump" in the solid curve at longitude 5 deg lies in the wake of the Oval BA, which contains transients. The longitude origin is shifted so it is always at the center of the Oval BA.**

Fletcher et al. [11] state while describing the commonly used calibration for observing Jovian temperatures, absolute temperatures are usually not determined, and therefore temporal changes in the temperature are usually not reported: "As pointed out by Orton et al. [12] and Simon-Miller et al. [13], this scaling technique renders the data insensitive to changes in the global mean temperatures of each planet between the Voyager (1979) and Cassini (2000) epochs."

Our hypotheses for the mechanism for transporting heat from the Jovian equator to its poles, for the disruption of that transport when the Oval BA formed, for a Jovian temperature change, and for the formation of the red annulus within the Oval BA are all controversial. Here, we show that all of the other published hypotheses for the Jovian heat transport that makes the cloud tops approximately isothermal from equator to pole and for the existence of the red annulus are problematic, while ours are plausible despite the lack of direct observational supporting evidence. Thus, the guiding principle of this paper is the words of Sherlock Holmes to Dr. Watson in the defense of his own deductions: "… and improbable as it is, all other explanations are more improbable still… How often have I said to you that when you have eliminated the impossible, whatever remains, however improbable, must be the truth?" [14,15]

In Sec. 1.1, we provide details of the unsolved problems of Jupiter's meridional heat transfer and in Sec. 1.2 we give details of the red annulus of the Oval BA. In Sec. 2, we review our hypothesized mechanism of meridional heat transport. In Sec. 3, we explain why observations of the Jovian clouds can be used as evidence that the 3D dynamics of the Oval BA did not change between the time it was formed and was white, and the time a red annulus appeared. In Sec. 4, we discuss the secondary circulation within the Oval BA and refer to our recent numerical results that examine secondary circulation (including the vertical velocity) of a radiatively damped 3D vortex like the Oval BA. Our explanation for the red annulus and why it requires a global temperature change on Jupiter is presented in Sec. 5, and our discussion is in Sec. 6.

**1.1 Heat Transport in the Jovian Weather Layer.** One of the most unusual findings of the Voyager spacecraft that flew by Jupiter in 1979 was that the temperature at the cloud-top level of the weather layer was nearly constant as a function of both longitude and latitude [16]. Jupiter's rapid rotation of approximately 10 h is much greater than the 4–5 y radiative time [17] of the weather layer, so it was not expected that the solar heating would make the temperature strongly dependent on longitude. However, most observers had expected that Jupiter's tropical latitudes, like those latitudes on Earth, would be warmer than its poles. Based on the increased solar flux striking the Jovian equator and the thickness, mean temperature, and radiative time scale of the layer, it had been expected that the equator would be approximately 30 K warmer than the poles [18]. However, Voyager observations showed that the longitudinally averaged temperature variations, based on the thermal emission fluxes at the cloud-top level, had only about a 4 K variation with latitude [2,19]. One proposed explanation for the nearly latitude-independent temperature of the weather layer was based on Jupiter's internal heating. Jupiter has an average (over the entire horizontal area of the weather layer) internal heat source of 5.7 Wm$^{-2}$ (compared with an average solar heating of 8.4 Wm$^{-2}$ [16,19]). Flasar proposed that an anisotropic internal heat source could cancel (to within 4 K) the inhomogeneity of the solar heating, but this explanation would require an extraordinary, and rather arbitrary, coincidence. (Jupiter's oblateness makes the gradient of its geopotential surface 7% larger in its polar direction than in its equatorial direction. A diffusive, heat-emitting Jovian core with coincident temperature and geopotential surfaces, and with a 7% oblateness would produce a poleward thermal flux 7% larger than the equatorial flux, but that anisotropic flux would not be great enough to balance the excess solar heating at the equator.)

To explain the uniformity of the cloud-top temperatures, Pirraglia [19] proposed that dynamical processes transported heat from the Jovian equator to its poles, but he did not attempt to model quantitatively any specific mechanism. He did propose that thermal convection played a role. Convection is very good at mixing heat both vertically, and in the case of a planetary atmosphere, meridionally, i.e., in the north–south direction. Assuming that the weather layer was fully convective, Ingersoll and Porco [20] computed the meridional Jovian heat transport using a mixing-length model of convection and found that the equator–pole temperature difference at the cloud-top level was less than 1 K. In their model, they assumed that the internal heat flux was uniform (and specifically, was not concentrated at the poles) and that the solar heating of the Jovian atmosphere was deposited at the elevations of the optically thick clouds, which they set at 1–2 bars. We agree with these last two assumptions and have incorporated them into our models discussed below. However in contrast to the model of Ingersoll and Porco, in our models the fully convective zone lies entirely beneath the weather layer and the elevations where the solar radiation is deposited. In the model of Ingersoll and Porco, since the inhomogeneous solar heating occurs at the same elevations where the convection is vigorous, it is not surprising that their temperatures showed little variation with latitude. In contrast in our models of the weather layer, convection cannot vigorously mix heat (although there may be some local mixing of heat due to small intermittent convective storms). Therefore, it is not surprising that unless a new mechanical stirring is introduced into the weather layer (see Sec. 2) that our models have the Jovian poles significantly cooler than the equator.

The reason we believe that the weather layer is globally baroclinically and convectively stable is that so many long-lived vortices exist there. When we carry out numerical experiments in

a convective layer, they fail to produce, long-lived, Jovian-like anticyclones, such as the GRS and the Oval BA, whereas in our numerical experiments in a convectively stable layer, the vortices thrive [21]. In fact, we know of *no* numerical simulations by any group that create long-lived Jovian-like anticyclones in vigorously convective layers. Most published studies of the Jovian vortices use 2-dimensional models, such as the shallow-water (cf. [22]) or quasi-geostrophic equations (cf. [23,24]). These 2D models apply only to convectively stable layers as they require real values of the Brunt–Väisälä frequency. Thus, these 2D calculations all implicitly assume that the weather layer is globally convectively stable. Three-dimensional calculations of the long-lived Jovian vortices by others have also used convectively stable layers. Simulations of the GRS by Cho et al. [25] were carried out using a convectively stable quasi-geostrophic model; 3D simulations of the long-lived Jovian vortices and other coherent features in the Jovian atmosphere have been carried out with codes that require that the atmosphere is stable to convection. For example, the EPIC code [26] was used by Morales-Juberias et al. [27] to simulate the White Ovals, and that code, derived from a shallow-water code, requires a convectively stable (or neutral) atmosphere. Thus, we argue that the top of the Jovian convective zone is below the bottom of Jupiter's weather layer where the solar radiation is deposited. In addition to these arguments, other authors have stated that the bottoms of Jupiter's visible vortices and other features are not only below 2 bars, where almost no solar radiation penetrates the visible clouds [28], but also below 3–4 bars where there is virtually no penetration of solar photons even in cloud-free regions [29]. For example, 3D simulations by Showman and Dowling [30] of the Jovian "hot spots" at 7°N assume that the top of the convective zone is below 5 bars as indicated by their choice of the elevation for the bottom boundary of their domain for computing hot spots. They state, "We place the model bottom [of our computational domain] near 5 bars because latent heat effects are expected to generate a stable layer [above a height] starting at about that altitude." Other observations that support our argument that the top of the convective zone is below 4 bars are the persistent, bright, 5 $\mu$m, infrared arcs south of the GRS and Oval BA. These arcs are bright in the infrared because they, unlike the surrounding atmosphere, are cloud free down to the 4–7 bars elevation that is the source of the 5 $\mu$m radiation. Presumably, the cloud-free region arcs are a product of the interactions of the zonal flows with the vortices, which indicates that the vortices (and therefore the stable weather layer) extend down to 4–7 bars [31]. Thus, we argue that Jupiter's weather layer, where the solar energy is deposited, is convectively stable and that thermal convection is not responsible for the transport of energy from the equator to its poles. We agree with the pioneering calculations of Stone [18], who showed that a mechanical stirring mechanism *within the weather layer* itself is needed to account for the meridional transport of energy that makes the cloud-top temperatures at the Jovian poles nearly equal to the temperature at the equator. In Sec. 2, we argue that the chaotic advection of heat from the latitudinal meanderings of Jupiter's large vortices is that mechanism.

After the lecture upon which this paper is based was given, a detailed calculation of the temperatures in the upper Jovian troposphere was carried out by Liu and Schneider [32]. They used a general circulation model to compute flow velocities as well as the temperature. The goal of their study was to compute the zonal, east–west, flows of Jupiter, rather than understanding Jovian heat transport, but their results are relevant here. Their simulations show a pole–equator temperature difference of 10 K, which is higher than the observed value, but smaller than the 30 K difference if there were no meridional transport of heat by advection. A goal of their study was to understand Jupiter's prograde (eastward) equatorial jet, which they argue was created by the large amount of angular momentum transport toward the equator by large-amplitude Rossby waves. It is possible that these waves (and their associated turbulence) are also responsible for the meridional heat flux that lowers the equator–pole temperature difference in their simulations to 10 K. However, our own observations of Jupiter's velocity in its weather layer do not show evidence of large-amplitude Rossby waves [33,34]. In addition, the simulations of Liu and Schneider do not produce long-lived *anticyclones* such as the GRS or the Oval BA, which dominate the observations of the Jovian weather layer (and which we argue in Sec. 2 are important in heat transport), but rather show persistent *cyclones*. Moreover, the top of the convective zone (which we define as the height in the atmosphere where the average Brunt–Väisälä frequency is zero) in their simulations is at ~600 mbar (see their Fig. 5), which we have argued is too high.

**1.2 The Persistent Red Annulus of Oval BA.** Between 1998 and 2000, a row of anticyclonic vortices called the White Ovals with diameters of order several thousand kilometers near latitude 33°S on Jupiter merged together to form a single vortex called Oval BA [35,36]. Mergers of large vortices on Jupiter are rare (although a similar set of mergers near 33°S were observed during the 1930 s [37]). After its formation and until December 2005, the cloud tops of Oval BA were white like those of the clouds of the vortices from which it formed, but then a large annulus inside the vortex turned red, leaving its core and exterior white (Figs. 1 and 2). The causes of the mergers in 1998–2000 were analyzed by Youssef and Marcus [38] and Morales-Juberias et al. [39] but not the color change. To determine the cause of the color change, we developed a new method for determining the horizontal wind velocities in the Jovian weather layer by analyzing the cloud displacements in time sequences of spacecraft images. The method, called *advection corrected correlation image velocimetry* (ACCIV) assumes that the Jovian clouds are passive tracers and uses correlation image velocimetry [40,41] as its starting point. ACCIV is able to find velocity fields with uncertainties as small as 3–5 m/s [7,8,42]. Precise velocities can be found with ACCIV because image pairs separated by as much as ~10 h intervals can be used in the velocimetry, whereas previous automated correlation methods failed to work when the cloud image pairs were separated by more than 2 h (and therefore contained only small cloud displacements). Figure 2 illustrates the fact that we found that the velocity of the Oval BA was unchanged (to within the velocity uncertainty) between 2000 when it was all white, and 2006 when it contained the red annulus.

Like most other aspects of this paper, our finding that the horizontal velocity of the Oval BA did not change is controversial. Simon-Miller et al. [43] and Cheng et al. [44] report large velocity changes in the Oval BA between 2000 and 2006. However, they used a manual extraction method to derive the velocities in which individual cloud features were identified by "eye" and traced between images. The finding by Simon-Miller et al. that the velocity of the Oval BA increased between 2000 and 2006 is based on the fact that the maximum velocity vector that they extracted from the cloud images increased from 120 m/s in 2000 to 180 m/s in April 2006. While it remains debatable whether a manual or automated method is better for determining velocities, we note that Simon-Miller et al. extracted fewer than 100 velocity vectors and that the maximum separation between image pairs was 83 min (with some separations as small as 41 min). They reported that the uncertainty in their velocities was 70 m/s (which is larger than that they reported maximum change in velocity between 2000 and 2006). Our ACCIV analysis in Fig. 2 used the same set of Hubble space telescope (HST) images taken in 2006 that were used by Simon-Miller et al. but we extracted ~63, 000 independent velocity vectors with uncertainties between 3 and 5 m/s. It is possible that the highest velocity vector within the Oval BA did increase between 2000 and 2006, and it is also possible that ACCIV underreports the speeds of the highest velocities due to its inherent spatial averaging (which is about a distance of 235 km for the HST images used in Figs. 1 and 2, compared with the 163 km effective resolution of the HST images and the 8000 km diameter of the Oval BA [42]). However, as pointed out by ourselves [42] and

others [45], in making the determination of whether the winds of the Oval BA changed from 2000 to 2006, changes in the overall azimuthal velocity along Oval's east–west axis—as shown in Fig. 2 and along other radial "spokes" of the Oval (as shown in Fig. 3 in Ref. [46]) are much better indications of a change in the winds of the Oval BA than the change in the value of its single highest velocity vector. The latter value has a much larger uncertainty than the average azimuthal velocity profile. In addition, it is possible that the value of the instantaneous maximum velocity of a Jovian vortex has an inherently large temporal variability and changes on times scales of weeks or days, as well as on a 6-yr time scale.

Cheng et al. [44] also observed that the peak velocity of the Oval BA had increased after the red annulus formed. They also used a manual method for extracting velocities, but they used images taken with the New Horizons spacecraft in 2007. Choi et al. [47] also used images from New Horizons, but they used a correlation method to obtain their velocities. Choi et al. also found that the velocities had increased from 2000, but by less than half the amount reported by Simon-Miller et al. and Cheng et al. The time separation between the New Horizon images was only 30 min [47]. Hueso et al. [45] used a correlation method to examine the velocities of the Oval BA in 2000 from Cassini images, in 2005 and 2006 from HST images, and in 2007 from New Horizon images. They reported that the value of the maximum velocity vector of the Oval BA was the same in 2000, 2005, and 2007 at 135 m/s and that in 2006 it was 130 m/s, with the differences being due to observational uncertainties. They state, "Our detailed measurements of the circulation of BA show that its velocity field did not change appreciably between its formation in 2000 and the latest high-resolution data-set in 2007." They also report that the extracted velocities are very sensitive to navigational errors in the images. They state that the navigational errors can be especially large in the New Horizons images used by Cheng et al. and Choi et al. "because the image sequence does not contain any portion of the planetary limb and the quality of the navigation of the image cannot be tested adequately."

In 2006 [7,8], we asked the question: if the horizontal velocities (and size and shape), i.e., the dynamics of the Oval BA did not change between 2000 and 2006, what caused the red annulus to form? Our hypothesis was that a global temperature change caused the color change. The hypothesis was elaborated upon in more recent publications [31,46]. The conclusion that the color change of the Oval BA was not due to a change in its dynamics was supported by Hueso et al. [45] who wrote "The internal motions in BA were indeed very similar to those previously found in the White Ovals that formed BA. From this analysis, the color change experienced in late 2005 seems not directly coupled to a change in the dynamics of the vortex and more subtle explanations are required."

New research that we carried out after the lecture, upon which this paper is based, makes it necessary for us to provide a warning to the reader. The lack of change in the horizontal velocities, shapes, and size of the Oval BA at its cloud-top level does not directly prove that all of the Oval's dynamical properties were unchanged between 2000 and 2007. In general, specifying the horizontal velocity of a 3D vortex at one elevation does not uniquely specify the vortex. In particular, vortices with different vertical thicknesses could have the same approximate appearance and velocities at their cloud-top levels. This is an important issue because one explanation of the red annuls of the Oval BA is that its vertical thickness increased so that it dredged up red material (or chemicals that could produce red material) from a deeper layer in the atmosphere [43]. There is observational evidence based on the haze above the Oval BA that the elevation of its top boundary did not change [48], but there is no direct evidence that the bottom boundary of the Oval BA is not now at a deeper elevation. Perez-Hoyos et al. [48] and other modelers of Jovian vortices [49,25] (and also modelers of persistent ocean vortices—see Ref. [50]) frequently cite the claim that quasi-geostrophic 3D vortices in a rotating stratified fluid have a vertical aspect ratio (characteristic vertical thickness to characteristic horizontal length scale) equal to $f/\bar{N}$ where $f$ is the Coriolis parameter of the latitude of the vortex and $\bar{N}$ is the ambient Brunt–Väisälä frequency at the latitude and elevation of the vortex. If that claim were correct and if there were no change in $\bar{N}$ between 2000 (which is believed both by us and by those who believe that there have been no global temperature changes), then $f/\bar{N}$ is unchanged. Thus, if the horizontal scale of the Oval BA was observed not to have changed (as shown in Fig. 2), then the vertical thickness and the elevation of the bottom boundary of the Oval BA would also be unchanged. However, our recent work shows that the aspect ratio of quasi-geostrophic vortices is not equal to $f/\bar{N}$ and that the aspect ratio also depends on other parameters [51,50]. Fortunately, as we explain in Sec. 3, those other parameters can be observed.

## 2 Chaotic Mixing of Heat

Jupiter's weather layer is dominated by a set of alternating, east–west jet streams and long-lived vortices [52]. We suggested [53] that the vortices are not just randomly scattered throughout the layer but tend to form rows or Kármán vortex streets of alternating cyclones and anticyclones that straddle each of Jupiter's westward-going jet streams. The three White Ovals that created the Oval BA were part of the Kármán vortex street centered at 34°S. Jupiter's anticyclones are much easier to detect in the cloud patterns than the cyclones, and its vortex streets are much easier to see in the southern hemisphere than in the northern. The vortices in the street are not stationary but slowly meander in longitude. We carried out two sets of two-dimensional numerical calculations to determine whether chaotic advection from the velocities of the meandering Kármán vortex streets could account for the large meridional transport of heat from the Jovian equator to its poles as implied by the nearly isothermal cloud tops.

We adopted a 2D (horizontal) version of the model heat equation used by Ingersoll and Porco [20]

$$\rho\, c_P \partial T/\partial t = \rho\, c_P[-(\mathbf{v}\cdot\nabla)T + \kappa\nabla^2 T] + [F_S\cos\theta - \sigma T^4 + F_B]/h \tag{1}$$

where $T$ and $\rho$ are the vertically averaged temperature and density of the weather layer, $c_P$ is the specific heat at constant pressure, $\mathbf{v}$ is the horizontal velocity in the weather layer, $\theta$ is the latitude, $F_S$ is longitudinally averaged solar heat flux, $F_B$ is the flux from below the weather layer, $\sigma$ is the Stefan–Boltzmann constant, $h$ is the thickness of the weather layer, $\kappa$ is a thermal diffusivity, and $\nabla^2$ is the horizontal Laplacian. Here, as in Ref. [20], we artificially replace the radiative transfer within the weather layer with a thermal diffusivity. We computed Eq. (1) in a doubly periodic Cartesian domain. We chose the value of $h\kappa$ to make the temperature $T(\theta)$ difference between the pole and the equator 30 K when $\mathbf{v} = \partial/\partial t = 0$ (i.e., steady, diffusive equilibrium). We first reported our solutions of this equation in Ref. [8]. Of course, the steady-state temperature solution to Eq. (1) is the same whether $\mathbf{v}$ is set to zero or set to the values of the east–west velocity of the Jovian zonal winds (which, by definition of *zonal* have no north–south component) because the inhomogeneous forcing term in Eq. (1) is independent of longitude $\phi$ and the steady-state temperature solution of Eq. (1) is independent of $\phi$ (thus, $(\mathbf{v}\cdot\nabla)T \equiv 0$).

In the first set of calculations, we set $\mathbf{v}$ in Eq. (1) equal to the steady-state equilibrium velocity $\mathbf{v}_{steady}$ of a model Jovian velocity that included both the east–west winds and Kármán vortex streets that straddled each of the model's 12 westward-going jet streams. Each Kármán vortex street consisted of six, equally spaced (in longitude) vortices (three cyclones interspersed with three anticyclones). The model winds were computed using the quasi-geostrophic equations as in Ref. [54]. The areas and strengths of the model vortices were chosen to be the same as the White Ovals from which Oval BA formed. Thus, the characteristic north–south

velocities of the vortices were of order 50 m/s, while the east–west jet stream velocities were of order 100 m/s. With only six vortices per westward-going jet stream most of the computational domain was not in a vortex, so it was not surprising that the advective heat flux $-\rho c_P(\mathbf{v}\cdot\nabla)T$ in Eq. (1) due to the vortices was relatively small, and that the late time, approximately steady, longitudinally averaged equilibrium temperature was not very different from the solution computed with $\mathbf{v}=0$ and had a ~25 K difference between pole and equator.

In the second set of calculations, the velocity was chaotic in time. When the equally longitudinally spaced vortices in the Kármán vortex streets are perturbed from their initial locations, they oscillate back-and-forth in longitude. When two opposite-signed vortices approach each other, they effectively repel and reverse direction. Usually, two opposite-signed vortices do not repel, but when they are embedded in alternating jet streams, the interaction between the vortices causes them to shift their locations in latitude. Those changes in latitude, coupled with the fact that the zonal winds vary with latitude, result in the vortices repelling each other [53]. To compute a temporally chaotic flow $\mathbf{v}_{chaos}$, we initialized our initial-value code with $\mathbf{v}_{steady}$ plus a small perturbation (which was created by displacing the initial locations of the anticyclones northward and the cyclones southward from the latitudes they had in the computation of $\mathbf{v}_{steady}$). The vortices in this simulation retained their initial circulations and oscillated in longitude. The frequency of the oscillations of the vortices is a function of the initial perturbation, and we chose the perturbation so that the period of the oscillations was ~12 y to match the observed periods of the oscillations of the White Ovals [37]. The flow was weakly chaotic. When we set the velocity equal to $\mathbf{v}_{chaos}$ in Eq. (1), we found that the meridional heat flux was greatly enhanced with the late-time, longitudinally and time-averaged temperature difference between the poles and the equator reduced to 6 K from 30 K, and consistent with Jovian observations. The increased transport of heat due to the advection from $\mathbf{v}_{chaos}$ was not surprising because it has been long established that even a weak chaotic flow can greatly enhance mixing and heat transport [55].

To consider what might have occurred when the three White Ovals near latitude 33°S merged into the anticyclone Oval BA, we repeated the initial-value calculation that we used to find $\mathbf{v}_{chaos}$, but this time we initialized the flow so that there was only one, rather than three, cyclone–anticyclone pair near 33°S. The anticyclone and cyclone near 33°S remained nearly equally spaced in longitude at all times, and the resulting velocity field $\mathbf{v}_{merged}$ near 33°S was nearly steady in time (and not chaotic). When the temperatures were recomputed with Eq. (1) with the velocity set equal to $\mathbf{v}_{merged}$, the north–south heat transport was efficient at the latitudes containing three pairs of vortices but was nearly blocked at latitude 33°S. The temperatures at latitudes just north of 34°S became 5–10 K warmer, and on the southern side they became cooler. These experiments motivated our conjecture in 2004 [4] that the mergers of the three White Ovals at 33°S would result in warming at Jovian longitudes north of 34°S and that the warming would begin approximately one thermal time, or 4–5 yr, after the vortex mergers formed the Oval BA. Thus, our prediction was that warming and observable indications of it might begin in the year 2005. Note that vortex mergers per se will not block the north–south heat transport; small vortex mergers occur frequently on Jupiter. The blockage of heat was due to the fact that the mergers of the White Ovals in 1998–2000 left the Kármán vortex street at 34 deg with only one anticyclone–cyclone pair, whose interactions did not produce sufficiently strong chaotic velocities.

## 3 Inferred Three-Dimensional Properties and Changes of the Oval BA

Here, we show that by measuring the 2D velocities at the elevation of the clouds of the Oval BA, we can characterize the 3D properties of the vortex including its vertical thickness. Thus, we shall be able to conclude that because the 2D velocities did not change between 2000 and 2006, neither did the thickness of the Oval BA. We can further conclude that since neither the upper boundary [48] nor the vertical thickness of Oval BA changed, the coloring of the red annulus in the Oval BA was *not* due to new material dredged into the Oval BA because its lower boundary moved to a lower elevation in the atmosphere.

Most publications that discuss the relationship between the characteristic vertical half-thickness of a Jovian vortex $D$ and its characteristic horizontal length $R$ employ Charney's quasi-geostrophic relation [56] that $D/R=f/\bar{N}$ [25,49,50]. If this relation were correct, then an unchanged $(f/\bar{N})$ and $R$ would show that the $D$ of Oval BA had not changed. However, we can show [51] that $D/R=f/\bar{N}$ violates the thermal wind equation [57]. Moreover, it implies that all vortices at the same latitude in an atmosphere, where $\bar{N}$ is a function only of latitude must have the same aspect ratio D/R regardless of the vortex's own properties such as its Rossby number Ro or internal Brunt–Väisälä frequency $N_c$. We recently showed in a combined analytic, numerical, experimental, and observational (using Atlantic meddies) study [51,50] that $D/R\neq f/\bar{N}$ and that this expression can be incorrect by two orders of magnitude. The correct relationship for the aspect ratio of a vortex, like a Jovian vortex, in a rotating stratified flow is

$$\left(\frac{D}{R}\right)^2=\frac{\mathrm{Ro}[1+(R/R_v)\mathrm{Ro}]}{N_c^2-\bar{N}^2}f^2 \tag{2}$$

where $R_v$ is the radius of the vortex. (Note that $R$ is defined to be the characteristic length associated with the horizontal derivative of the horizontal velocity [51]. For "hollow" vortices like the GRS in which the centers are nearly irrotational [58,59], $R_v\neq R$. However, for vortices like the Oval BA, $R_v\simeq R$.) For anticyclones, Ro is negative. From Eq. (2), to show that $D$ of the Oval BA did not change, it is necessary to show that $\bar{N}$, $N_c$, Ro, $R$, and $R_v$ did not change. Figure 2 (and Fig. 3 in Wong et al. [46]) shows that the last three quantities did not change between 2000 and 2006. The profile of the azimuthal velocity of a vortex as a function of the average radial distance to the vortex center can be used to derive the values of $\bar{N}$ and $N_c$, and using these profiles their values have been computed [58,59]. Because the horizontal velocity profiles did not change between 2000 and 2006, neither did $N_c$ and $\bar{N}$. Thus, $D$ did not change.

We can heuristically derive Eq. (2) for a quasi-geostrophic vortex with $R=R_v$, like the Oval BA. In this analysis, quantities with an over-bar are the equilibrium values in the ambient atmosphere far from the vortex. Quantities with a subscript "c" are the values along the central vertical axis of the vortex. An upper case delta $\Delta$ in front of a quantity indicates its "anomalous" value, defined as $\Delta Q(z)\equiv Q|_c-\bar{Q}$. The height $z$ where the vortex's azimuthal velocity has its maximum value is defined as $z_0$. Atmospheric stratification is parameterized with the Brunt–Väisälä frequency $N$ defined by

$$N^2\equiv(g/c_P)(\partial s/\partial z) \tag{3}$$

where $g$ is gravity and $s$ is the entropy [57]. The Oval's characteristic circumferential velocity at $z_0$ is $v_\perp$; the Rossby number is $\mathrm{Ro}\equiv v_\perp/|f|R$. The top and bottom of the vortex, located at $z_+$ and $z_-$, are defined to be the elevations where the vortex's horizontal circumferential velocity is effectively zero. The half-heights of the upper and lower parts of the vortex are $D_\pm\equiv|z_\pm-z_0|$. (See Fig. 3.) We use the notation that $Q_0\equiv\bar{Q}(z_0)$, $Q_\pm\equiv\bar{Q}(z_\pm)$, $\Delta Q_0\equiv\Delta Q(z_0)$, and $\Delta Q_\pm\equiv\Delta Q(z_\pm)$.

A quasi-geostrophic anticyclone, like the Oval BA, with $|\mathrm{Ro}|\leq 1$ has a high pressure core $\Delta P$ confined horizontally by the Coriolis force [57]. Identifying the Oval's $z_0$ with the cloud elevation where the horizontal velocities were extracted gives

Ro $\simeq -0.147$. Thus, $\Delta P$ is determined by geostrophic balance in the horizontal momentum equation [57]

$$\nabla P \simeq \rho_c f(\mathbf{v} \times \hat{\mathbf{z}})[1 + O(\mathrm{Ro})] \tag{4}$$

where $\nabla$ is the horizontal component of the gradient, $\hat{\mathbf{z}}$ is the vertical unit vector, and $\mathbf{v}$ is the velocity. Equation (4) implies

$$\Delta P_0 \simeq \rho_0 |f| v_\perp R > 0; \quad \Delta P_\pm = 0 \tag{5}$$

The second equality in Eq. (5) is due to the geostrophic balance in Eq. (4): locations where the horizontal circumferential velocity is zero, i.e., at $z = z_\pm$, must have $\Delta P = 0$. Vertical hydrostatic equilibrium requires $d(\Delta P)/dz = -g\Delta\rho$. Thus, in the vertical direction, the high pressure core is confined hydrostatically by high and low density anomalies located at the top $z_+$ and bottom $z_-$ of the vortex, so

$$\Delta\rho_\pm = \frac{\pm(\Delta P_0)}{gD_\pm} \tag{6}$$

$$= \frac{\pm|f|\rho_0 v_\perp R}{gD_\pm} \tag{7}$$

where Eq. (7) is obtained by eliminating $\Delta P_0$ from Eq. (6) with Eq. (5). By definition, the circumferential horizontal velocity has its maximum at $z_0$; therefore, Eq. (4) shows that at $z_0$, $d(\Delta P)/dz = 0$. The vertical hydrostatic balance equation shows that $(\Delta\rho) = 0$ at $z_0$. Using Eq. (3) and the definition of $\Delta$, we obtain

$$\bar{N}^2 - N_c^2 = \frac{-g}{c_P}\frac{d(\Delta s)}{dz} \simeq \frac{g}{\rho_0}\frac{d(\Delta\rho)}{dz} \simeq \pm\frac{g}{\rho_0}\frac{(\Delta\rho)_\pm}{D_\pm} \tag{8}$$

where the approximations in Eq. (8) are valid for an ideal gas. Eliminating $\Delta\rho_\pm$ from Eqs. (7) and (8) and using the definition of the Rossby number Ro, we obtain Eq. (2) in the geostrophic limit (i.e., ignoring the quadratic terms in the Rossby number). Note that the equilibrium vortex has temperature anomalies. From the ideal gas equation

$$(\Delta T)_\pm/T_0 = (\Delta P)_\pm/P_0 - (\Delta\rho)_\pm/\rho_0 \tag{9}$$

so an anticyclone has a cool dense top and a warm buoyant bottom, with the opposite anomalies for a cyclone.

## 4 Secondary Circulation Within an Anticyclone

We have shown numerically that an anticyclone in a protoplanetary disk (with an ideal gas equation of state) that is slowly decaying due to a weak radiative dissipation causes a secondary flow in the anticyclone like the one in Fig. 3 [60]. We have numerically observed similar secondary circulations for radiatively decaying anticyclones in a Boussinesq fluid. Shortly after Voyager observed Jupiter in 1979, Conrath et al. [49] speculated that there was an upwelling along the central axis in the upper part of Jovian White Ovals like the upwelling in Fig. 3. Their speculation was based on the observation that the visible clouds at the centers of the White Ovals were cooler than the ambient atmosphere. They argued that the cool anomalies were created by rising plumes (that conserved entropy as they rose along the central axes in the upper parts of the vortices). Because the atmosphere was stably stratified (i.e., subadiabatic), the rising plumes would adiabatically cool and create the observed cold anomalies.

Based on the work of Conrath et al. and our own numerical experiments of decaying vortices, we speculated that a radiatively damped anticyclone, like the Oval BA, *that does not decay*, but is kept approximately steady by some type of mechanical forcing will have a secondary circulation like the one in Fig. 3 [61,62,31,46]. Many authors believe that the persistent Jovian vortices survive much longer than the radiative thermal damping

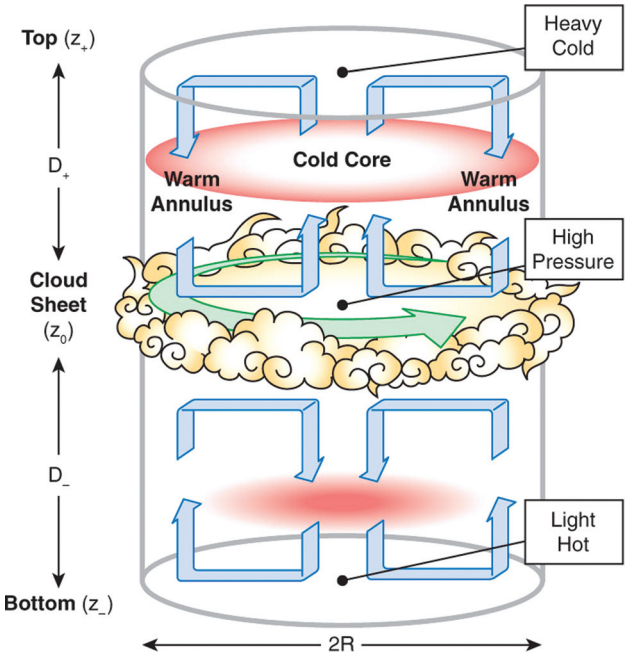


**Fig. 3 Schematic of the Oval's primary circumferential (green, or counterclockwise, arrow in the middle of the figure) and secondary circulations (blue arrows, or the arrows with vertical components). The primary flow is zero at the Oval's top and bottom and is assumed to be greatest near the cloud elevation where the horizontal velocities were extracted (at the cloud sheet at $z_0$). In the Oval's upper part, the secondary circulation rises along the central vertical axis, cooling the gas, and it descends in an annulus near the Oval's outer radial edge creating a warm annulus there. The flow in the Oval's bottom part mirrors the flow in the top part. Red shading (or the shading near the top and bottom of the figure) denotes the warm annulus in the Oval's top part and the warm core in the Oval's bottom.**

time of 4–5 y because they are sustained by their frequent mergers with smaller vortices [63,64].

Our speculation that the secondary circulation in Fig. 3 applies to vortices like the Oval BA cannot be tested because no one has yet produced numerically or experimentally a 3D simulation of a radiatively damped, but mechanically sustained, anticyclone. However, the motivation for our speculation is as follows. In our numerical studies of a weakly radiatively damped anticyclone, the magnitudes of the temperature anomalies $(\Delta T)_\pm$ decay by radiation. Because the pressure anomalies are not affected by radiation, the magnitudes of the density anomalies $(\Delta\rho)_\pm$ decrease in accord with Eq. (9). This creates an imbalance in the vertical hydrostatic equilibrium because the unchanged central pressure anomaly $\Delta P_0$ is too strong for the underdense vortex top and the underbuoyant vortex bottom. This imbalance causes the anticyclone to slowly "explode" with vertical velocities along the central axis like those shown in Fig. 3. The explosion is slow and not violent because the vertical velocity advects potential density (entropy) so that the overdensity of the top of the vortex is partially restored, i.e., in a compressible atmosphere the rising motion along the top central axis of the anticyclone adiabatically cools the flow at the top of the vortex which increases the overdensity there, bringing the vertical hydrostatic equation more nearly into balance.

We speculate that this same scenario occurs in a radiatively damped, but mechanically sustained, anticyclone. We speculate that the energy balance of a sustained anticyclone is as follows. Potential energy is removed from the anticyclone as mass is removed from its overdense top and added to its underdense bottom (i.e., $|(\Delta\rho)_\pm|$ decreases) through radiative decay of the temperature anomalies $|(\Delta T)_\pm|$. This potential energy is resupplied from the kinetic energy of the secondary circulation. In

particular, the vertical velocities along and near the vortex's central axis do mechanical work as they move potential density upward in the upper of the vortex and downward in the lower part of the vortex. The vertical velocity of the secondary flow is driven by the excessively high pressure anomaly at the vortex center. The pressure anomaly at the center is "excessively high" in the sense that it is higher than it would be if the vortex were in hydrostatic equilibrium with the density anomalies $(\Delta\rho)_{\pm}$. The kinetic energy of the secondary flow is resupplied from the primary azimuthal velocity of the vortex. The kinetic energy of the primary azimuthal velocity of the vortex is resupplied from the mergers with the small vortices.

We caution the reader that the schematic of the secondary flow in Fig. 3 looks deceptively like the secondary Ekman circulation in a viscously decaying anticyclone that is vertically confined between two no-slip boundaries. However, in the Jovian troposphere, there are no vertically confining no-slip boundaries (required by Ekman pumping), so any relationship between the secondary flow in Fig. 3 and Ekman circulation must be a coincidence. Secondary circulations within the Oval BA are *not* due to Ekman pumping. Moreover, we have shown numerically that viscous dissipation in a slowly decaying 3D vortex without vertical no-slip boundaries creates a secondary flow like the one in Fig. 3 but with the *opposite* sign [51,65,66]. To see why the sign of a secondary flow caused by viscous dissipation (or any mechanical or friction induced dissipation) is opposite in sign to one caused by radiative dissipation, consider the horizontal balance (5) and vertical balance Eq. (6). The horizontal balance equation shows that a viscous (or any other type of) decay in the magnitude of the primary azimuthal velocity $v_{\perp}$ produces a decrease in the anticyclone's central high pressure $\Delta P_0$ but leaves the density anomalies $\Delta\rho_{\pm}$ unchanged. The pressure decrease in the center of the anticyclone makes the vertical hydrostatic Eq. (6) out of balance. The reduced central pressure is unable to support the overdense vortex top and the overbuoyant vortex bottom, so the vortex slowly implodes with the vertical velocities along the central axis opposite in sign to those shown in Fig. 3. Thus, we believe that any published estimate of the magnitude of the *upward* vertical velocities in the top parts of the White Ovals or Oval BA based on the Ekman number, viscosity, eddy viscosity, or Rayleigh friction is not valid.

## 5 The Oval BA as a "Thermometer"—Explanation of the Red Annulus

The atmospheric coloring agent, or chromophore, that gives the red annulus of the Oval BA and the GRS their red colors is not known, cf. [46]. Nevertheless, we have an explanation for the red annulus in the Oval BA, and our explanation answers four critical questions: (1) Why was the red chromophore of the annulus not in Oval BA, or not visible within it prior to December 2005? (2) Why did the color of the Oval BA change five years after the Oval BA formed? (3) Why does the red color appear in an annular ring, as opposed, say, to the center of the vortex where the upwelling is strongest? (4) Why has the red color remained confined to the annular ring for over six years?

We proposed that the red annular ring of the Oval BA and the annulus in the top part of the vortex containing the downwelling secondary circulation in Fig. 3 are the same region [61,62]. The downwelling adiabatically heats the atmosphere in the annulus, and that small warming can have a large effect on colors. West et al., noting the seasonal color changes on Jupiter, proposed that Jovian clouds act as color-changing "thermometers" [67]. They suggested that Jupiter's red chromophores are solid particulates that coexist with ammonia vapor close to its saturation density. Cloud temperatures are approximately equal to the sublimation temperature of ammonia because Jupiter's visible cloud deck is, by definition, at the elevation where ammonia ice crystals first form in abundance and make the atmosphere optically thick. West et al. suggested that small temperature variations change the clouds' colors because a cooling causes white ammonia ice to mantle onto red particulates, hiding the red, and changing the cloud hues from red to white. Warming sublimates the ice, changing the hues from white to red during Jupiter's spring and summer. We argue that the visible white parts of the clouds of the Oval BA are heavily mantled with white ammonia ice, while the annulus of descending atmosphere is warm enough to sublimate the ammonia and expose the red nuclei.

This scenario answers the four questions posed above: (1) The nuclei containing the red chromophore along with the ammonia were always contained within the Oval BA and the three White Ovals from which it formed. No change in elevation of the bottom boundary or large vertical velocities was required to dredge red chromophores from a deeper level of the atmosphere. To make the red chromophore visible required only the sublimation of the ammonia ice that obscured it. (2) The time between the appearance of the red annulus and the time that the Oval BA formed (and the start of the blocking of the advection of heat from the equator to the south pole) is one thermal time of the atmosphere. After the heat transport was blocked near 34°S the atmospheric temperature, it took approximately one thermal time for the temperature of the atmosphere to respond. The temperature at the latitude of the Oval BA increased more than anywhere else on the planet and the warming affected the interior and exterior temperatures of the Oval BA equally (because the values of $(\Delta T)_{\pm}$ were set by geostrophic and hydrostatic balance—and therefore by the values of $R$ and $v_{\perp}$—and needed to remain constant to keep Oval BA in equilibrium). Prior to December 2005, the Oval BA was cool enough so that the red nuclei were mantled with enough ammonia ice to appear white everywhere. (3) The increase in temperature that started in 2000 was enough by the end of 2005 to sublimate the ammonia ice in the warmest part of the Oval BA, the downwelling atmosphere in the annulus, but not at other locations. Jovian vortices at other latitudes did not experience a large enough warming (or cooling) to change color. (4) The red color remains confined within the warm annulus despite that fact that fluid parcels, red particulates, and ammonia freely mix within the Oval BA, moving in and out of the warm annulus. Unlike the red-cored particulates and the gases in the atmosphere, the Oval's warm temperature anomaly does *not* advect with the flow, but remains tied to the downwelling so that the red color remains within the annulus. If the red color of the annulus were due to red particulates that entered or formed in the Oval BA after it was created in 2000, and if the color of those particulates were temperature-independent, then the Oval-BA would have turned entirely red after one horizontal mixing time of the atmosphere inside the Oval. (That mixing time is less than 2 yr based on a "turbulent mixing diffusivity" equal to $V_{\text{eddy}}\, L_{\text{eddy}}$, where $V_{\text{eddy}}$ and $L_{\text{eddy}}$ are the velocity and length of the characteristic turbulent eddies in the Oval BA, which observations suggest are as least as large as $\sim$3 m/s and $\sim$100 km, respectively). As noted by Wong et al. [46], our color change explanation for the Oval BA requires only that the color of the particulates change with temperature (with warm particulates red and cool particulates white). Thus, temperature-dependent color-changing chemistry, rather than ice mantling, could be responsible for the red annulus.

Our explanation of the red annulus is consistent with the fact that most patterns in clouds are ephemeral and are only semipermanent if they are attached to a fixed feature. For example on Earth, cloud features above mountainous islands are semipermanent because the upwelling caused by the mountains causes water condensation and cloud formation to reoccur at the same locations. Thus, the cloud pattern survives despite the fact that the individual components of the clouds are mixed and advected from the region by the ambient winds. On Jupiter, where the troposphere has no solid bottom boundary, long-lived cloud patterns such as the dark rings around the anticyclones at 41°S are tied to the outer edges of long-lived vortices [4]. Other small long-lived Jovian vortices at latitudes between 41°S and 65°S have visible rings in their clouds near the vortex boundaries (cf. Fig. 13 in [31]), while large long-lived Jovian vortices often have

bright infrared arcs just outside their boundaries (cf. Fig. 12 in Ref. [31]). We believe that downwelling in the upper part of the Oval BA shown schematically in Fig. 3 is the permanent feature that the cloud pattern of the red annulus is tied to.

## 6 Discussion

We have argued that there has been an overall warming of the Jovian troposphere at latitudes north of 34°S and a corresponding cooling in the southern latitudes. Our reasoning was based on two unexplained Jovian phenomena: the fact that the cloud top-temperatures are nearly the same at the Jovian equator and at its poles, and the appearance in 2005 of a red annulus within the Oval BA. Our conjecture that the north–south heat transport of Jupiter is greatly enhanced by the chaotic mixing of heat due to the chaotic motion of large Jovian vortices can be partially tested in future numerical experiments, but it will be difficult to prove. This is due to the fact that the computation of the heat transfer in the troposphere is intimately connected to the overall dynamics there that create and maintain the east–west winds. The theory and correct numerical modeling of those winds remain in dispute, cf. [32,68,69]. In addition, the importance of intermittent convection in the weather layer in the mixing of heat is not known.

On the other hand, the controversies surrounding the red annulus of the Oval BA will likely be settled in the near future due to better extractions and analyses of the horizontal winds of the Oval BA from cloud images. In addition, numerical simulations are advancing to the point where a 3D radiatively damped, but mechanically sustained, Jovian-like vortex can be computed. Then, quantitative numerical calculations, rather than the schematic in Fig. 3, can be used to study the secondary flows and temperature fields of the Oval BA and determine whether a red annulus can be created and made to persist.

## Acknowledgment

This work was supported by the NASA Planetary Atmospheres Program and by the NSF AST and ATI Programs. This work used an allocation of computer resources from the Extreme Science and Engineering Discovery Environment (XSEDE), which was supported by National Science Foundation Grant No. OCI-1053575. The observations of the Jovian clouds are associated with HST Programs GO/DD 10782 and GO 11102, with support provided by NASA through a grant from the Space Telescope Science Institute, which is operated by the Association of Universities for Research in Astronomy, Inc., under NASA Contract NAS 5-26555. We thank P. Hassanzadeh and C.-H. Jiang for help with the computer simulations.

## Nomenclature

$c_P$ = specific heat at constant pressure, J/(kg K)
$D$ = characteristic vertical half-thickness of a vortex, km
$D_-$ = vertical half-thickness of lower part of vortex, km
$D_+$ = vertical half-thickness of upper part of vortex, km
$F_B$ = heat flux from below the weather layer, $W/m^2$
$F_S$ = longitudinally averaged solar heat flux, $W/m^2$
$f$ = Coriolis parameter, 1/s
$g$ = Jovian acceleration of gravity at 1 bar, $m/s^2$
$h$ = vertical thickness of the weather layer, km
$\bar{N}$ = mean Brunt–Väisälä frequency, 1/s
$N_c$ = Brunt–Väisälä frequency at vortex center, 1/s
$P$ = pressure, $N/m^2$
$R$ = characteristic horizontal length of a vortex based on its velocity derivative, km
$R_v$ = average horizontal radius of a vortex, km
Ro = Rossby number
$s$ = entropy, J/(kg K)
$T$ = temperature, K
$\mathbf{v}$ = horizontal velocity, m/s
$\nu_\perp$ = characteristic circumferential velocity of a vortex, m/s
$z_0$ = vertical coordinate of vortex center, km
$z_-$ = vertical coordinate of vortex bottom, km
$z_+$ = vertical coordinate of vortex top, km
$\kappa$ = thermal diffusivity, $m^2/s$
$\rho$ = mass density, $kg/m^3$
$\sigma$ = Stefan–Boltzmann constant, $W/(m^2K^4)$
$\theta$ = latitude, deg

## References

[1] Gierasch, P. J., Ingersoll, A. P., Banfield, D., Ewald, S. P., Helfenstein, P., Simon-Miller, A., Vasavada, A., Breneman, H. H., Senske, D. A., and Galileo Imaging Team, 2000, "Observation of Moist Convection in Jupiter's Atmosphere," Nature, **403**, pp. 628–630.
[2] Gierasch, P. J., Conrath, B. J., and Magalhaes, J. A., 1986, "Zonal Mean Properties of Jupiter's Upper Troposphere From Voyager Infrared Observations," Icarus, **67**, pp. 456–483.
[3] Hooke, R., 1665, "A Spot in One of the Belts of Jupiter," Philos. Trans. R. Soc. London, **1**, p. 3.
[4] Marcus, P. S., 2004, "Prediction of a Global Climate Change on Jupiter," Nature, **428**, pp. 828–831.
[5] Marcus, P. S., and Youseff, A., 2001, "Mergers of Planetary Vortices and Their Consequences," BAPS 54th Annual Meeting of the Division Fluid Dynamics, No. BL.005.
[6] Marcus, P. S., 2002, "Using Vortex Dynamics to Predict an Impending Global Climate Change for Jupiter," BAPS 55th Annual Meeting of the Division of Fluid Dynamics, Vol. 47.
[7] Asay-Davis, X., Shetty, S., Marcus, P., de Pater, I., Lockwood, S., Wong, M., and Go, C. Y., 2006, "Extraction of Velocity Fields From HST Image Pairs of Jupiter's Great Red Spot, New Red Oval and Zonal Jet Streams," BAAS DPS, Vol. 38, No. 11.01.
[8] Shetty, S., Marcus, P., Asay-Davis, X., de Pater, I., Wong, M., Lockwood, S., and Go, C. Y., 2006, "Modeling and Data Assimilation of the Velocity Fields of Jupiter's Great Red Spot, New Red Oval and Zonal Jet Streams," BAAS DPS, Vol. 38, No. 11.03.
[9] Go, C. Y., de Pater, I., Wong, M., Lockwood, S., Marcus, P., Asay-Davis, X., and Shetty, S., 2006, "Evolution of the Oval BA During 2004-2005," BAAS DPS, Vol. 38, No. 11.02.
[10] Go, C. Y., de Pater, I., Rogers, J., Orton, G., Marcus, P., Wong, M. H., Yanamandra-Fischer, A., and Joels, J., 2007, "The Global Upheaval of Jupiter," BAAS DPS, Vol. 39, No. 19.09.
[11] Fletcher, L. N., Orton, G. S., Yanamandra-Fisher, P. A., Fisher, B. M., Parrish, P. D., and Irwin, P. G. H., 2009, "Retrievals of Atmospheric Variables on the Gas Giants From Ground-Based Mid-Infrared Imaging," Icarus, **200**, pp. 154–175.
[12] Orton, G. S., Friedson, A. J., Caldwell, J., Hammel, H. B., Baines, K. H., Bergstralh, J. T., Martin, T. Z., Malcom, M. E., West, R. A., Golisch, W. F., Griep, D. M., Kaminski, C. D., Tokunaga, A. T., and Shure, R. B. M., 1991, "Thermal Maps of Jupiter's Spatial Organization and Time Dependence of Stratospheric Temperatures, 1980 to 1990," Science, **252**, pp. 537–542.
[13] Simon-Miller, A. A., Poston, A., Orton, G. S., and Fisher, B., 2007, "Wind Variations in Jupiter's Equatorial Atmosphere: A QQO Counterpart?," Icarus, **186**, pp. 192–203.
[14] Doyle, S. A. C., 1893, "Silver Blaze," *The Memoirs of Sherlock Holmes*, G. Newnes Ltd, London.
[15] Doyle, S. A. C., 1890, "The Sign of the Four," Lippincott's Monthly Magazine, London.
[16] Flasar, F. M., 1986, "Global Dynamics and Thermal Structure of Jupiter's Atmosphere," Icarus, **65**, pp. 280–303.
[17] Gierasch, P. J., and Goody, R. M., 1969, "Radiative Time Constants in the Atmosphere of Jupiter," J. Atmos. Sci., **26**, pp. 979–980.
[18] Stone, P. H., 1972, "A Simplified Radiative-Dynamical Model for the Static Stability of Rotating Atmospheres," J. Atmos. Sci., **29**, pp. 405–418.
[19] Pirraglia, J. A., 1984, "Meridional Energy Balance of Jupiter," Icarus, **59**, pp. 169–176.
[20] Ingersoll, A. P., and Porco, C. C., 1978, "Solar Heating and Internal Heat Flow on Jupiter," Icarus, **35**, pp. 27–43.
[21] Marcus, P. S., 1988, "Numerical Simulation of Jupiter's Great Red Spot," Nature, **331**, pp. 693–696.
[22] Dowling, T. E., and Ingersoll, A. P., 1989, "Jupiter's Great Red Spot as a Shallow Water System," J. Atmos. Sci., **46**(21), pp. 3256–3278.
[23] Ingersoll, A. P., and Cuong, P. G., 1981, "Numerical Model of Long-Lived Jovian Vortices," J. Atmos. Sci., **38**(10), pp. 2067–2076.
[24] Dowling, T. E., and Ingersoll, A. P., 1988, "Potential Vorticity and Layer Thickness Variations in the Flow Around Jupiter's Great Red Spot and White Oval BC," J. Atmos. Sci., **45**, pp. 1380–1396.
[25] Cho, J. Y.-K., de la Torre Juarez, M., Ingersoll, A. P., and Dritschel, D. G., 2001, "High-Resolution, Three-Dimensional Model of Jupiter's Great Red Spot," J. Geophys. Res., **106**(E3), pp. 5099–5105.
[26] Dowling, T. E., Fisher, A. S., Gierasch, P. J., Harrington, J., Jr., Lebeau, R. P., and Santori, C. M., 1998, "The Explicit Planetary Isentropic-Coordinate (EPIC) Atmospheric Model," Icarus, **132**, pp. 221–238.

[27] Morales-Juberias, R., Sanchez-Lavega, A., and Dowling, T. E., 2003, "EPIC Simulations of the Meger of Jupiter's White Ovals BE and FA: Altitude-Dependent Behavior," Icarus, **166**(1), pp. 63–74.
[28] Simon-Miller, A. A., Banfield, D., and Gierasch, P. J., 2001, "Color and the Vertical Structure in Jupiter's Belts, Zones, and Weather Systems," Icarus, **154**(2), pp. 459–474.
[29] Sromovsky, L., and Fry, P., 2002, "Jupiter's Cloud Structure as Constrained by Galileo Probe and HST Observations," Icarus, **157**(2), pp. 373–400.
[30] Showman, A. P., and Dowling, T. E., 2000, "Nonlinear Simulations of Jupiter's 5-Micron Hot Spots," Science, **289**, pp. 1737–1740.
[31] de Pater, I., Wong, M., Marcus, P., Luszcz-Cook, S., Ádámkovics, M., Conrad, A., Asay-Davis, X., and Go, C., 2010, "Persistent Rings in and Around Jupiter's Anticyclones–Observations and Theory," Icarus, **210**, pp. 742–762.
[32] Liu, J., and Schneider, T., 2010, "Mechanisms of Jet Formation on the Giant Planets," J. Atmos. Sci., **67**, pp. 3652–3672.
[33] Asay-Davis, X., Marcus, P., Wong, M., and de Pater, I., 2009, "Jupiter's Shrinking Great Red Spot and Steady Oval BA: Velocity Measurements With the 'Advection Corrected Correlation Image Velocimetry' Automated Cloud-Tracking Method," Icarus, **203**, pp. 164–188.
[34] Asay-Davis, X., Marcus, P., Wong, M., and de Pater, I., 2011, "Changes in Jupiter's Zonal Velocity Between 1979 and 2008," Icarus, **211**, pp. 1215–1232.
[35] Sanchez-Lavega, A., Rojas, J., Hueso, R., Lecacheux, J., Colas, F., Acarreta, J., Miyazaki, I., and Parker, D., 1999, "Interaction of Jovian White Ovals BC and DE in 1998 From Earth-Based Observations in the Visual Range," Icarus, **142**(1), pp. 116–124.
[36] Sanchez-Lavega, A., Orton, G., Morales, R., Lecacheux, J., Colas, F., Fisher, B., Fukumura-Sawada, P., Golisch, W., Griep, D., Kaminski, C., Baines, K., Rages, K., and West, R., 2001, "The Merger of Two Giant Anticyclones in the Atmosphere of Jupiter," Icarus, **149**(2), pp. 491–495.
[37] Rogers, J. H., 1995, *The Giant Planet Jupiter*, Cambridge University Press, Cambridge.
[38] Youssef, A., and Marcus, P. S., 2003, "The Dynamics of Jovian White Ovals From Formation to Merger," Icarus, **162**, pp. 74–93.
[39] Morales-Juberias, R. A., Sanchez-Lavega, A., and Dowling, T. E., 2003, "EPIC Simulations of the Merger of Jupiter's White Ovals BE and FA: Altitude-Dependent Behavior," Icarus, **166**, pp. 63–64.
[40] Fincham, A. M., and Spedding, G. R., 1997, "Low Cost, High Resolution DPIV for Measurement of Turbulent Fluid Flow," Exp. Fluids, **23**, pp. 449–462.
[41] Fincham, A. M., and Delerce, G., 2000, "Advanced Optimization of Correlation Imaging Velocimetry Algorithms," Exp. Fluids, **29**, pp. 13–22.
[42] Asay-Davis, X. S., 2009, "Jupiter's Shrinking Great Red Spot and Steady Oval BA: Velocity Measurements With the Advection Corrected Correlation Image Velocimetry Automated Cloud Tracking Method," Icarus, **203**, pp. 164–188.
[43] Simon-Miller, A. A., Chanover, N. J., Orton, G. S., Sussman, M., Tsavaris, I. G., and Karkoschka, E., 2006, "Jupiter's White Oval Turns Red," Icarus, **185**, pp. 558–562.
[44] Cheng, A. F., Simon-Miller, A. A., Weaver, H. A., Baines, K. H., Orton, G. S., Yanamandra-Fisher, P. A., Mousis, O., Pantin, E., Vanzi, L., Fletcher, L. N., Spencer, J. R., Stern, S. A., Clarke, J. T., Mutchler, M. J., and Noll, K. S., 2008, "Changing Characteristics of Jupiter's Little Red Spot," Astron. J., **135**, pp. 2446–2452.
[45] Hueso, R., Legarreta, J., Garcia-Melendo, E., Sanchez-Lavega, A., and Perez-Hoyos, S., 2009, "The Jovian Anticyclone BA II. Circulation and Interaction With the Zonal Jets," Icarus, **203**, pp. 499–515.
[46] Wong, M., de Pater, I., Asay-Davis, X., Marcus, P. S., and Go, C., 2011, "Vertical Structure of Jupiter's Oval BA Before and After it Reddened: What Changed?," Icarus, **215**, pp. 211–225.
[47] Choi, D. S., Showman, P., and Vasavada, A. R., 2007, "The Evolving Flow of Jupiter's White Ovals and Adjacent Cyclones," Icarus, **207**, pp. 359–372.
[48] Perez-Hoyos, S., Sanchez-Lavega, A., Hueso, R., Garcia-Melendo, E., and Legarreta, J., 2009, "The Jovian Anticyclone BA III. Aerosol Properties and Color Change," Icarus, **203**, pp. 516–530.
[49] Conrath, B. J., Flasar, F. M., Pirraglia, J. A., Gierasch, P. J., and Hunt, G. E., 1981, "Thermal Structure and Dynamics of the Jovian Atmosphere: 2. Visible Cloud Features," J. Geophys. Res., **86**(A10), pp. 8769–8775.
[50] Aubert, O., Le Bars, M., Le Gal, P., and Marcus, P. S., "The Universal Aspect Ratio of Vortices in Rotating Stratified Flows: Experiments and Observations," J. Fluid Mech., **706**, pp. 34–45.
[51] Hassanzadeh, P., Marcus, P. S., and Le Gal, P., "The Universal Aspect Ratio of Vortices in Rotating Stratified Flows: Theory and Simulation," J. Fluid Mech., **706**, pp. 46–57.
[52] Smith, B. A., Soderblom, L. A., Johnson, T. V., Ingersoll, A. P., Collins, S. A., Shoemaker, E. M., Hunt, G. E., Masursky, H., Carr, M. H., Davies, M. E., Cook, A. F., Boyce, J., Danielson, G. E., Owen, T., Sagan, C., Beebe, R. F., Veverka, J., Strom, R. G., McCauley, J. F., Morrison, D., Briggs, G. A., and Suomi, V. E., 1979, "The Jupiter System Through the Eyes of Voyager 1," Science, **204**, pp. 951–972.
[53] Marcus, P. S., 1993, "Jupiter's Great Red Spot and Other Vortices," Annu. Rev. Astron. Astrophys., **31**, pp. 523–573.
[54] Humphreys, T., and Marcus, P. S., 2007, "Vortex Street Dynamics: The Selection Mechanism for the Areas and Locations of Jupiter's Vortices," J. Atmos. Sci., **64**, pp. 1318–1333.
[55] Ottino, J. M., 1997, *The Kinematics of Mixing: Stretching, Chaos, and Transport*, Cambridge University Press, Cambridge.
[56] Charney, J. G., 1971, "Geostrophic Turbulence," J. Atmos. Sci., **28**, pp. 1087–1095.
[57] Kundu, P. K., 1990, *Fluid Mechanics*, Academic Press, San Diego, CA.
[58] Shetty, S., Asay-Davis, X. S., and Marcus, P. S., 2007, "On the Interaction of Jupiter's Great Red Spot and Zonal Jet Streams," J. Atmos. Sci., **64**, pp. 4432–4444.
[59] Shetty, S., and Marcus, P., 2010, "Changes in Jupiter's Great Red Spot (1979–2006) and Oval BA (2000–2006)," Icarus, **210**, pp. 182–201.
[60] Barranco, J., and Marcus, P. S., 2005, "Three-Dimensional Vortices in Stratified Protoplanetary Disks," Astrophys. J., **623**, pp. 1157–1170.
[61] Marcus, P., Asay-Davis, X., Shetty, S., de Pater, I., Wong, M., Lockwood, S., and Go, C. Y., 2006, "Velocities and Temperatures of Jupiter's Great Red Spot and the New Red Oval and Their Implications for Global Climate Change," BAAS DPS, Vol. 38.
[62] Marcus, P. S., Shetty, S., and Asay-Davis, X., 2006, "Velocities and Temperatures of Jupiter's Great Red Spot and the New Red Oval and Implications for Global Climate Change," BAPS 59th Annual Meeting of the Division of Fluid Dynamics, Vol. 51.
[63] Ingersoll, A. P., Beebe, R. F., Mitchell, J. L., Garnea, G. W., Yagi, G. M., and Muller, J. P., 1981, "Interaction of Eddies and Mean Zonal Flow on Jupiter as Inferred From Voyager 1 and 2 Images," J. Geophys. Res., **86**(A10), pp. 8733–8743.
[64] Salyk, C., Ingersoll, A. P., Lorre, J., Vasavada, A., and Genio, A. D. D., 2006, "Interaction Between Eddies and Mean Flow in Jupiter's Atmosphere: Analysis of Cassini Imaging Data," Icarus, **185**, pp. 430–442.
[65] Pei, S., Hassanzadeh, P., and Marcus, P. S., 2010, "Secondary Flows Within 3D Vortices," BAPS 63rd Annual Meeting of the Division of Fluid Dynamics, Vol. 55.
[66] Hassanzadeh, P., Pei., S., and Marcus, P. S., 2010, "How do 3D Vortices Spin Down, or Do They?," BAPS 63rd Annual Meeting of the Division of Fluid Dynamics, Vol. 55.
[67] West, R. A., Strobel, D. F., and Tomasko, M. G., 1986, "Clouds, Aerosols, and Photochemistry in the Jovian Atmosphere," Icarus, **65**, pp. 161–217.
[68] Heimpel, M., Aurnou, J., and Wicht, J., 2005, "Simulation of Equatorial and High-Latitude Jets on Jupiter in a Deep Convection Model," Nature, **438**, pp. 193–196.
[69] Sayanagi, K. M., Showman, A. P., and Dowling, T. E., 2008, "The Emergence of Multiple Robust Zonal Jets From Freely Evolving, Three-Dimensional Stratified Geostrophic Turbulence With Applications to Jupiter," J. Atmos. Sci., **65**, pp. 3947–3962.